

PHYSICS

Unprecedented high irreversibility line in the nontoxic cuprate superconductor $(\text{Cu,C})\text{Ba}_2\text{Ca}_3\text{Cu}_4\text{O}_{11+\delta}$ Yue Zhang¹, Wenhao Liu¹, Xiyu Zhu^{1,2*}, Haonan Zhao¹, Zheng Hu¹, Chengping He¹, Hai-Hu Wen^{1,2*}

One of the key factors that limit the high-power applications for a type II superconductor is the irreversibility line $H_{\text{irr}}(T)$, which reflects the very boundary of resistive dissipation in the phase diagram of magnetic field versus temperature. In cuprate family, the Y-, Bi-, Hg-, and Tl-based systems have superconducting transition temperatures exceeding the liquid nitrogen boiling temperature (~ 77 K). However, the toxic elements Hg and Tl in the latter two systems strongly constrain the applications. The best perspective so far is relying on the $\text{YBa}_2\text{Cu}_3\text{O}_{7-\delta}$ ($T_c \approx 90$ K) system, which is nontoxic and has a relatively high irreversibility magnetic field. We report the study of a nontoxic superconductor $(\text{Cu,C})\text{Ba}_2\text{Ca}_3\text{Cu}_4\text{O}_{11+\delta}$ with $T_c = 116$ K. We found that the irreversibility magnetic field is extremely high, and it thus provides great potential for applications above the liquid nitrogen temperature.

INTRODUCTION

For a type II superconductor, the magnetic field will penetrate into the sample and form quantized vortices when the external magnetic field is beyond a threshold H_{c1} . This state, with the mixture of superconducting area and magnetic vortices, is called as the mixed state. The upper boundary of the mixed state is the upper critical magnetic field H_{c2} at which the Cooper pairs are completely absent (within the Bardeen-Cooper-Schrieffer picture). However, for a superconductor to carry the nondissipative supercurrent, another boundary, namely, the irreversibility line $H_{\text{irr}}(T)$, is very crucial. This phase line actually separates the phase diagram into zero and finite resistive dissipation. In the cuprate family, some compounds of the Bi-based (1), Hg-based (2), and Tl-based (3) systems show superconducting transition temperatures beyond 100 K. Among all these materials, it was reported that the $(\text{Tl}_{0.5}\text{Pb}_{0.5})\text{Sr}_2\text{Ca}_2\text{Cu}_3\text{O}_9$ [(Tl,Pb)-1223] (4, 5) exhibits a rather high irreversibility line with an irreversibility field of nearly 10 T at the liquid nitrogen boiling temperature (~ 77 K), which is thought to be promising for applications. However, for Hg- and Tl-based systems, the toxic elements Hg and Tl strongly limit the high-power applications of these materials. The nontoxic Bi-based $[\text{Bi}_2\text{Sr}_2\text{Ca}_2\text{Cu}_3\text{O}_{10+\delta}]$ (Bi-2223), $T_c \approx 110$ K system also has a transition temperature exceeding 100 K, but the very layered structure and huge anisotropy do not allow a high irreversibility field at the liquid nitrogen temperature (6, 7). The irreversibility field and superconducting current density decrease rapidly with increasing temperature in the moderate temperature region. For the nontoxic $\text{Bi}_2\text{Sr}_2\text{CaCu}_2\text{O}_8$ system, the material can be made into round wire, and the irreversibility field is high at the liquid He temperature; therefore, it could lead to the high magnetic field applications at low temperatures (8). The Y-based $\text{YBa}_2\text{Cu}_3\text{O}_{7-\delta}$ (YBCO; $T_c \approx 90$ K), which is nontoxic and has a high irreversibility field (about 8 to 10 T at 77 K) (9, 10), is thought to be a promising material for applications. By irradiation, the first-order melting of vortex lattice in YBCO are turned into a second-order transition, but the irreversibility line does

not change too much (11). Actually, on the basis of the material $\text{HgBa}_2\text{Ca}_3\text{Cu}_4\text{O}_{10+\delta}$ (Hg-1234) with T_c of about 124 K (12), several nontoxic compounds in the formula of $\text{MBa}_2\text{Ca}_3\text{Cu}_4\text{O}_{11+\delta}$ with T_c of about 117 K were fabricated, here, $M = (\text{Cu,C})$ or Cu (13–15), etc. On the basis of the model analysis, for example, by assuming the very small anisotropy $\gamma = \xi_{ab}/\xi_c = 1.6$ in this system, Ihara (16) suggested a possibility of good performance of applications. Preliminary results of resistivity and magnetization were reported on this system (17–19), and the measured irreversibility fields at 77 K were much lower than the expected value (16). In present work, the synthesis and systematic measurements of resistivity and magnetization are reported in the nontoxic superconductor $(\text{Cu,C})\text{Ba}_2\text{Ca}_3\text{Cu}_4\text{O}_{11+\delta}$ [(Cu,C)-1234] with $T_c = 116$ K, which exhibits, as far as we know, the highest irreversibility line so far among all superconductors in the liquid nitrogen temperature region in terms of practical applications. This statement is made on the basis of the comparison of $H_{\text{irr}}(T)$ between our polycrystalline samples of (Cu,C)-1234 and other systems (including polycrystalline samples, or thin films and crystals with $H \parallel c$ axis). It is found that the irreversibility field $\mu_0 H_{\text{irr}}$ of (Cu,C)-1234 made in this work reaches about 15 T at 86 K and 5 T at 98 K, providing a great chance of high-power applications in the temperature region of 100 K.

RESULTS

X-ray diffraction pattern, magnetization, and resistivity measurements of sample 1

The (Cu,C)-1234 bulk samples were made by solid-state reaction method under high pressure and high temperature. The details of synthesis and characterization are given in Materials and Methods and the Supplementary Materials. We conducted the resistivity and magnetization measurements with the Quantum Design instruments PPMS16T (physical property measurement system 16 T) and SQUID-VSM7T (superconducting quantum interference device–vibrating sample magnetometer 7 T), respectively. The powder x-ray diffraction (XRD) pattern of sample 1 can be fit quite well with the standard (Cu,C)-1234 XRD pattern (fig. S4). It shows a dominant tetragonal (Cu,C)-1234 phase with a space group $P4/mmm$ with parameters $a = 3.86$ Å and $c = 17.94$ Å. The volume fraction that resulted from this fitting was about 93%. The main impurity phase is CaCuO_2

¹Center for Superconducting Physics and Materials National Laboratory of Solid State Microstructures and Department of Physics, Nanjing University, Nanjing 210093, China. ²Collaborative Innovation Center of Advanced Microstructures, Nanjing University, Nanjing 210093, China.

*Corresponding author. Email: zhuxiyu@nju.edu.cn (X.Z.); hhwen@nju.edu.cn (H.-H.W.)

(<7%), which is marked with green vertical lines below the spectrum. Two asterisks indicate the unknown phase, which takes a very small fraction of the sample.

Figure 1A shows the temperature-dependent resistivity of sample 1 under different magnetic fields. One can see that the superconducting transition occurs at about 116 K with a rather narrow transition width ($\Delta T_c \approx 1$ K) determined from the 10 to 90% normal-state resistivity. In the inset of Fig. 1A, we present the temperature dependence of magnetic susceptibility measured in zero-field-cooled (ZFC) and field-cooled (FC) modes for the as-synthesized sample 1 (Cu,C)-1234 under 10 Oe. A calculation of the magnetic screening volume using the ZFC data at 10 Oe is about 196%. The reason for the value larger than 100% is due to the demagnetization factor. Again, the diamagnetic susceptibility measurement shows a well-defined transition at about 116 K, being consistent with the resistivity measurements. It is important to emphasize that, without carbon involved in the last step of high-pressure and high-temperature sin-

tering, we could not reach superconductivity. It was claimed in previous reports that even pure Cu (without using carbon) could lead to superconductivity under the pressure of 5 GPa (13, 15). It is worth mentioning that the carbon may not go to the Cu positions on the CuO₂ planes. As revealed by neutron powder diffraction measurements and analysis, the carbon atoms in the form of CO₃ may occupy to the Cu position (which would be the Hg position in the Hg-1234) (20). It remains an interesting and open question how the carbon atoms are incorporated into the structure.

As shown in Fig. 1 (A and B), the superconducting transition becomes broad in the magnetic field, which is induced by the vortex motion. Since our sample is bulk, the crystallographic direction is random in different grains. It is reasonable to assume that the threshold of dissipation is determined by the grains with magnetic field parallel to *c* axis in some grains or the weak link areas. As we can see, the magnetic field-induced broadening is rather slow compared with the nontoxic Bi-2223 system. If a criterion of resistivity of 1% ρ_n (T_c) is chosen, as marked by the blue horizontal dashed line, then the determined irreversibility field is 15 T at about 82 K (Fig. 1B). With the same criterion, the irreversibility fields are about 3 T at 98.6 K and 5 T at 94.2 K. Actually, even higher values of irreversibility fields are found in another sample (sample 2). The irreversibility fields are 15 T at 86 K, 5 T at 98 K, and 3 T at 101.2 K (fig. S1). All these values suggest that the nontoxic system (Cu,C)-1234 may have the highest irreversibility line among all superconductors above the liquid N₂ temperature.

Magnetization hysteresis loops and critical current density of sample 1

To evaluate the intrinsic critical current density and its behavior in a magnetic field, we crushed the sample into powder with an average grain size of about 5 μm and measured the magnetization. We measured the averaged grain size using a scanning electron microscope (SEM; Hitachi Co. Ltd.; fig. S3). Then, we used the hydrochloric acid to corrode the surface of bulk sample 1 for a few seconds to show the grains. We measured the magnetization hysteresis loops (MHLs) of sample 1 in powder state from 4.2 to 110 K for applied fields up to 7 T (Fig. 2A). It is clear that the magnetization is irreversible up to quite high temperatures and magnetic fields. For the powdered superconducting sample, the critical current density J_c was determined by using the Bean critical-state model J_c (A/cm²) = $30\Delta M/d$ (18, 21), where ΔM (in units of electromagnetic unit per cubic centimeter) is the width of the MHL, and d (in units of centimeter) is the averaged size of the grains. Using Bean critical-state model, we obtain the critical current density J_c versus magnetic field at different temperatures (Fig. 2B). It is clear that the J_c value can reach about 6×10^6 A/cm² at 4.2 K at Earth's field. In addition, the critical current is quite robust in the presence of the magnetic field. Using a criterion of 1000 A/cm², we obtain an irreversibility field of about 2 T at 100 K, which is slightly lower than that determined from the resistive measurements because the criterion of J_c adopted here is rather high. At about 90 K, the critical current density J_c keeps flat versus magnetic field, indicating a much higher irreversibility magnetic field.

DISCUSSION

As shown above, the critical current density and the irreversibility line in the (Cu,C)-1234 system are both very high. Here, we

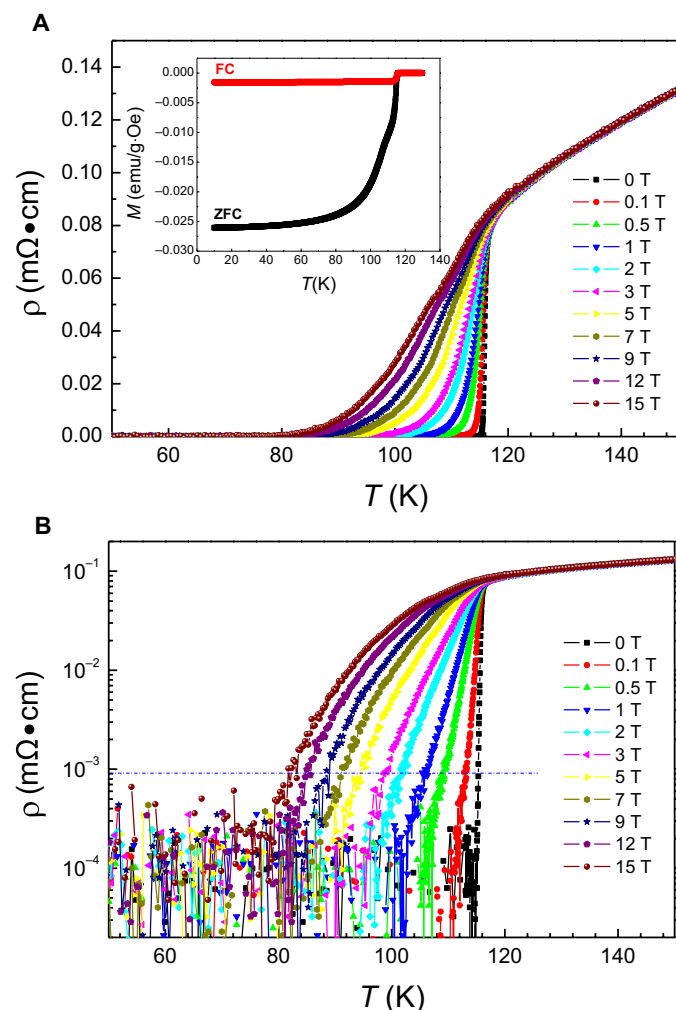


Fig. 1. Temperature dependence of resistivity and magnetization of sample 1. (A) Temperature dependence of resistivity under different magnetic fields from 0 to 15 T. The inset shows the temperature dependence of magnetic susceptibility measured in ZFC and FC modes under a magnetic field of 10 Oe. (B) The same data in (A) in the semilogarithmic scale. The blue horizontal dashed line represents the criterion of resistivity 1% ρ_n (T_c), which is used to determine the irreversibility line.

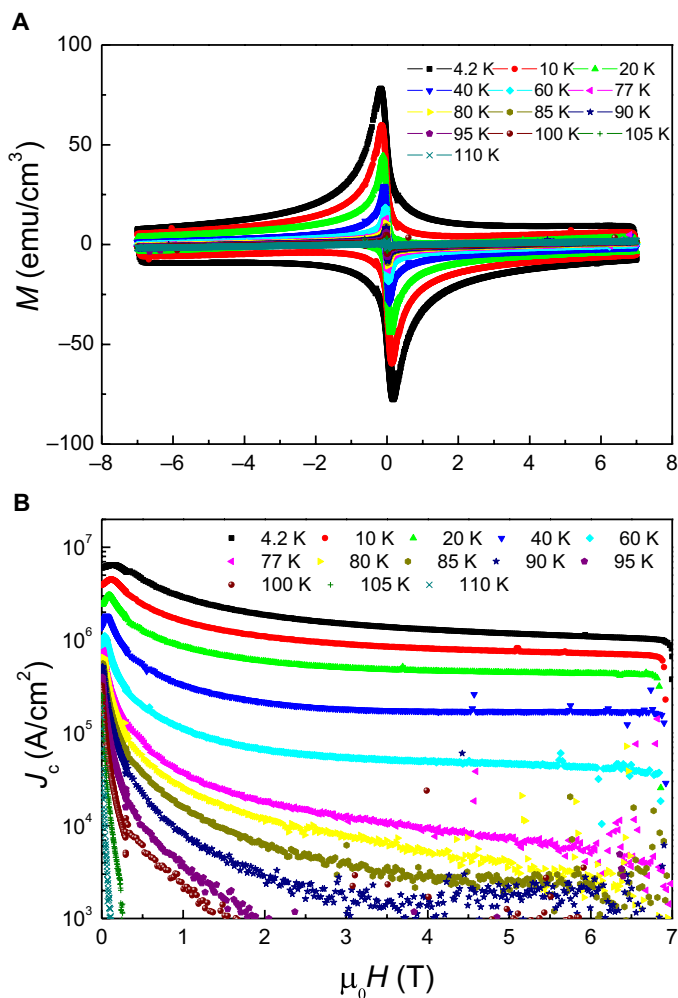


Fig. 2. Magnetization and critical current density of powdered sample (sample 1). (A) MHLs of high pressure synthesized (Cu,C)-1234 from 4.2 to 110 K under magnetic fields up to 7 T. (B) Field dependence of critical current density J_c at various temperatures. J_c is determined by the formula $J_c (\text{A/cm}^2) = 30\Delta M/d$, where d (in units of centimeter) is the averaged grain size of the powder sample. Some strongly scattered data are the bad points during the SQUID measurements on powdered samples. Because of the presence of an unphysical hysteresis background in our SQUID-VSM measurements corresponding to a small current density, we have deducted the background $\log(J_c) = 0.295H + 1.84$ from the data, with J_c in units of amperes per square centimeter and H in tesla.

would like to give a comparison of the irreversibility lines in different cuprate systems. It is worth noting that the irreversibility line of sample 1 is obtained by using a resistivity criterion of $1\% \rho_n$ ($\rho_n \approx 0.09$ milliohm-cm), as shown by the dashed blue line in Fig. 1B, which is also adopted by other groups. Figure 3 shows the comparison of irreversibility lines for (Cu,C)-1234 (samples 1 and 2 in this work), YBCO (single crystals) (9, 10), Bi-2223 (thin film) (6), Bi-2223 (single crystal) (7), and (Tl,Pb)-1223 (5). It is clear that the nontoxic Bi-2223 has a very low irreversibility field at 77 K, while YBCO has a relatively high $\mu_0 H_{\text{irr}}$ (about 8 to 10 T at 77 K, $H \parallel c$ axis) compared with Bi-2223. The material (Tl,Pb)-1223 shows a higher T_c and irreversibility line than YBCO while it contains the toxic element Tl. However, the irreversibility field of the nontoxic samples (Cu,C)-1234 synthesized in this work shows a much steeper temperature

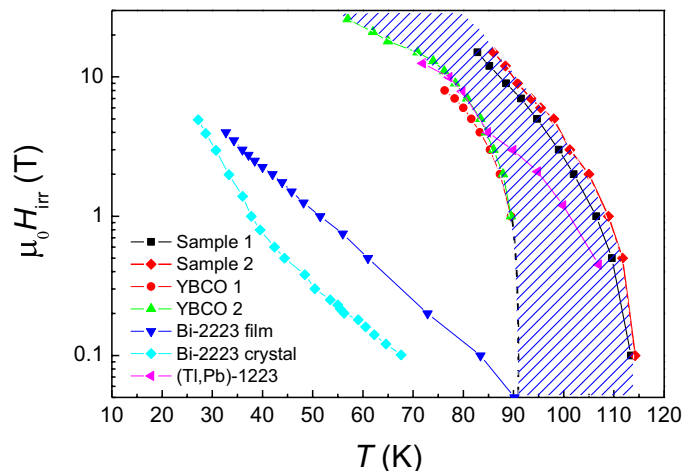


Fig. 3. Irreversibility lines of different cuprate systems. Irreversibility lines for (Cu,C)-1234 (this work, sample 1 and sample 2), YBCO 1 and YBCO 2 (single crystals, $H \parallel c$ axis) (9, 10), Bi-2223 (thin film, blue down triangles) (6), Bi-2223 (single crystal, cyan diamond) (7), and (Tl,Pb)-1223 (pink triangles) (5). The highlighted area indicates the region for zero dissipation above the boundary of YBCO. The black dashed line shows the trend of irreversibility line of YBCO with $T_c = 91$ K.

dependence near T_c . In previous studies, the magnetizations were measured for samples of the same system (Cu,C)-1234 (17–19) or $\text{AuBa}_2\text{Ca}_3\text{Cu}_4\text{O}_{11}$ (Au-1234) (22), but the irreversibility lines reported there are not as high as our samples. This may be induced by the difference of the material morphologies inside the sample. We have gone through the literature that we could collect for the Hg- or Tl-based systems, including that for Hg-1212 (23), Hg-1223 (24), Hg-1234 (25), and Tl-1223 (26), and found that none of these materials has the irreversibility line beyond the present system (Cu,C)-1234. For films and crystals, the data when $H \parallel c$ axis are used for comparison, since it is believed that the critical current density with magnetic field parallel to c axis or the weak links limit the irreversibility lines in the polycrystalline samples. From the literature, one can find that the irreversibility fields at 77 K are ~ 4 T (Hg-1212) (23), ~ 6 T (Hg-1223) (24), ~ 2 T (Hg-1234) (25), and ~ 3 T (Tl-1223) (26), which are below the values of our present sample. We also checked the infinite layer system $(\text{Sr}_{1-x}\text{Ca}_x)_{1-y}\text{CuO}_2$ with $T_c \approx 110$ K (27), and there is quite little data about the irreversibility lines of this system perhaps because most of the samples have not been made to a perfect state. From the available data in one of the infinite layer $\text{Sr}_{0.9}\text{La}_{0.1}\text{CuO}_2$ ($T_c = 43$ K) (28), one can see that the anisotropy is not very small and the irreversibility line is also quite low. As mentioned already, there is an irreversibility field of 15 T at 82 K for sample 1; it even shoots up to 15 T at 86 K in sample 2. Here, in Fig. 3, we use the highlighted area to indicate the region with finite supercurrent (or zero/weak resistive dissipation) of our sample as compared with YBCO. One can see that there is a large area beyond the irreversibility line of YBCO where the samples can carry nondissipative supercurrent, providing great potential for applications in the temperature region of 100 K. It should be emphasized that the present samples were made through the high-pressure synthesis. The present results just show very good intrinsic properties for application of the nontoxic material (Cu,C)-1234 and related systems. It is highly desired to try new methods with lower pressure or thin-film deposition to make the superconducting wire/tape based on this promising material. The presently used techniques for fabricating the coating conductor of

YBCO, such as ion bombardment–assisted deposition (29, 30), rolling-assisted biaxially textured substrates (31, 32), and metal-organic chemical vapor deposition, etc., may also be tried for this material. Comparing the critical current densities presented in Fig. 2 in the case of the grains and fig. S2 in the case of the bulk crystalline sample, one can see a difference of two orders of magnitude. This implies that the connectivity between the grains of the polycrystalline bulk is strongly degraded and the currents cannot circulate very well over the whole bulk sample. If this weak link problem in the bulk polycrystalline can be improved or eliminated, then it will be promising to make round wires by using this material. The discovery reported in this work will stimulate new efforts in the practical applications based on this material system.

MATERIALS AND METHODS

Sample growth and characterization

The bulk samples were made using the solid-state reaction method under high pressure and high temperature using the appropriate precursors $\text{BaCuO}_{2.13}$ and Ca_2CuO_3 . The precursor $\text{BaCuO}_{2.13}$ was obtained by calcining BaO_2 and CuO at 900°C in flowing oxygen gas for a total duration of 60 hours, intermittently grinding twice in the interests of homogeneity. The precursor Ca_2CuO_3 was prepared first by calcining a well-ground mixture of CaCO_3 and CuO at 950°C in air for 20 hours, and then the obtained Ca_2CuO_3 powder was sintered in flowing oxygen gas at 950°C for 40 hours with one or two intermediate grinding. The process of making Ca_2CuO_3 was in an open environment; therefore, the carbon can escape, and the amount of carbon is not counted in the precursor Ca_2CuO_3 . The carbon in the final sample is thus introduced only in the next step of high-pressure and high-temperature sintering process. After mixing and grinding different components with molar ratios of $1.8\text{BaCuO}_{2.13}$, $1.4\text{Ca}_2\text{CuO}_3$, 0.2CaCO_3 , 0.2BaCO_3 , 1.2CuO , and appropriate amount of $0.8\text{Ag}_2\text{O}$ (used as oxidizer), the mixture was pressed into a pellet with the nominal formula of $(\text{Cu}_{0.4}\text{C}_{0.4})\text{Ba}_2\text{Ca}_3\text{Cu}_4\text{O}_{11+\delta}$. This pellet was sealed into a gold capsule for the final step of high-pressure and high-temperature synthesis. For high-pressure synthesis, the sample enclosed by gold capsule was placed into a BN container, surrounded by graphite sleeve resistance heater and pressure transmitting MgO rods. The final reaction was carried out at 1100° to 1150°C under 3.5 GPa for 1 to 2 hours and then cooled down to room temperature in 5 minutes before the pressure was released. The chemical analysis was performed on some grains by using energy dispersive x-ray spectrum based on SEM (Phenom ProX), and the results are shown in fig. S5. The statistics show that the carbon exists in all grains with the molar ratio of 0.3 to 0.4 per formula of (Cu,C) -1234, being consistent with the stoichiometry of the pellet before the last step sintering. The compositions from the analysis are really close to the nominal ones of the pellet before the last step sintering under high pressure and high temperature.

Resistivity, magnetization, and XRD measurements

Resistivity, magnetization, and XRD were measured on the samples. The dc magnetic susceptibility was measured using a Quantum Design instrument SQUID-VSM7T. Magnetization hysteresis loop measurement was performed with magnetic fields up to 7 T. The resistivity versus temperature with magnetic fields from 0 to 15 T was measured by the standard four-probe method using a physical property measurement system (PPMS16T, Quantum Design). The XRD was

measured using a Bruker D8 Advanced diffractometer with the $\text{CuK}\alpha_1$ radiation at room temperature.

SUPPLEMENTARY MATERIALS

Supplementary material for this article is available at <http://advances.sciencemag.org/cgi/content/full/4/9/eaau0192/DC1>

Fig. S1. Resistivity and magnetization versus temperature of sample 2.

Fig. S2. Magnetization and critical current density of sample 2 in bulk form.

Fig. S3. SEM image of the surface after being treated by hydrochloric acid of sample 1.

Fig. S4. Powder XRD pattern for sample 1.

Fig. S5. SEM images and composition analysis on fresh surface of sample 1.

REFERENCES AND NOTES

1. H. Maeda, Y. Tanaka, M. Fukutomi, T. Asano, A new high- T_c oxide superconductor without a rare earth element. *Jpn. J. Appl. Phys.* **27**, L209 (1988).
2. A. Schilling, M. Cantoni, J. D. Guo, H. R. Ott, Superconductivity above 130 K in the Hg–Ba–Ca–Cu–O system. *Nature* **363**, 56–58 (1993).
3. Z. Z. Sheng, A. M. Hermann, Bulk superconductivity at 120 K in the Ti–Ca/Ba–Cu–O system. *Nature* **332**, 138–139 (1988).
4. R. S. Liu, D. N. Zheng, J. W. Loram, K. A. Mirza, A. M. Campbell, P. P. Edwards, High critical-current densities in $(\text{Th}_{0.5}\text{Pb}_{0.5})\text{Sr}_2\text{Ca}_2\text{Cu}_3\text{O}_9$ with T_c up to 115 K. *Appl. Phys. Lett.* **60**, 1019–1021 (1992).
5. D. N. Zheng, A. M. Campbell, R. S. Liu, P. P. Edwards, Critical current, magnetic irreversibility line and relaxation in a single Ti–O layers 1223 superconductor. *Cryogenics* **33**, 46–49 (1993).
6. Q. Li, M. Suenaga, T. Kaneko, K. Sato, C. Simmon, Collapse of irreversible field of superconducting $\text{Bi}_2\text{Sr}_2\text{Ca}_2\text{Cu}_3\text{O}_{10+\delta}/\text{Ag}$ tapes with columnar defects. *Appl. Phys. Lett.* **71**, 1561–1563 (1997).
7. N. Clayton, N. Musolino, E. Giannini, V. Garnier, R. Flükiger, Growth and superconducting properties of $\text{Bi}_2\text{Sr}_2\text{Ca}_2\text{Cu}_3\text{O}_{10}$ single crystals. *Supercond. Sci. Technol.* **17**, S563–S567 (2004).
8. J. Y. Jiang, H. P. Miao, Y. B. Huang, S. Hong, J. A. Parrell, C. Scheuerlein, M. D. Michiel, A. K. Ghosh, U. P. Trociewitz, E. E. Hellstrom, Reduction of gas bubbles and improved critical current density in Bi-2212 round wire by swaging. *IEEE Trans. Appl. Supercond.* **23**, 6400206 (2013).
9. A. M. Petrean, L. M. Paulius, W.-K. Kwok, J. A. Fendrich, G. W. Crabtree, Experimental evidence for the vortex glass phase in untwinned, proton irradiated $\text{YBa}_2\text{Cu}_3\text{O}_{7-\delta}$. *Phys. Rev. Lett.* **84**, 5852–5855 (2000).
10. T. Nishizaki, T. Naito, N. Kobayashi, Anomalous magnetization and field-driven disordering transition of a vortex lattice in untwinned $\text{YBa}_2\text{Cu}_3\text{O}_y$. *Phys. Rev. B* **58**, 11169–11172 (1998).
11. W. K. Kwok, L. M. Paulius, V. M. Vinokur, A. M. Petrean, R. M. Ronningen, G. W. Crabtree, Vortex pinning of anisotropically splayed defects in $\text{YBa}_2\text{Cu}_3\text{O}_{7-\delta}$. *Phys. Rev. Lett.* **80**, 600–603 (1998).
12. E. V. Antipov, S. M. Loureiro, C. Chaillout, J. J. Capponi, P. Bordet, J. L. Tholence, S. N. Putilin, M. Marezi, The synthesis and characterization of the $\text{HgBa}_2\text{Ca}_2\text{Cu}_3\text{O}_{8+\delta}$ and $\text{HgBa}_2\text{Ca}_3\text{Cu}_4\text{O}_{10+\delta}$ phases. *Physica C* **215**, 1–10 (1993).
13. H. Ihara, K. Tokiwa, H. Ozawa, M. Hirabayashi, A. Negishi, H. Matuhata, Y. S. Song, New high- T_c superconductor family of Cu-Based $\text{Cu}_{1-x}\text{Ba}_2\text{Ca}_{n-1}\text{Cu}_n\text{O}_{2n+4-\delta}$ with $T_c > 116$ K. *Jpn. J. Appl. Phys.* **33**, L503–L506 (1994).
14. T. Kawashima, Y. Matsui, E. Takayama-Muromachi, New oxycarbonate superconductors $(\text{Cu}_{0.5}\text{C}_{0.5})\text{Ba}_2\text{Ca}_{n-1}\text{Cu}_n\text{O}_{2n+3}$ ($n = 3, 4$) prepared at high pressure. *Physica C* **224**, 69–74 (1994).
15. C.-Q. Jin, S. Adachi, X.-J. Wu, H. Yamauchi, S. Tanaka, 117 K superconductivity in the Ba–Ca–Cu–O system. *Physica C* **223**, 238–242 (1994).
16. H. Ihara, How to achieve the best performance superconductor based on Cu-1234. *Physica C* **364–365**, 289–297 (2001).
17. H. Kumakura, H. Kitaguchi, K. Togano, T. Kawashima, E. Takayama-Muromachi, S. Okayasu, Y. Kazumata, Flux pinning and irreversibility lines of new oxycarbonate superconductors $(\text{Cu}_{0.5}\text{C}_{0.5})\text{Ba}_2\text{Ca}_{n-1}\text{Cu}_n\text{O}_{2n+3}$ ($n = 3, 4$) and $(\text{Cu}_{0.5}\text{C}_{0.5})_2\text{Ba}_3\text{Ca}_{n-1}\text{Cu}_n\text{O}_{2n+3}$ ($n = 3, 4$). *IEEE Trans. Appl. Supercond.* **5**, 1399–1404 (1995).
18. H. Kumakura, K. Togano, T. Kawashima, E. Takayama-Muromachi, Critical current densities and irreversibility lines of new oxycarbonate superconductors $(\text{Cu}_{0.5}\text{C}_{0.5})\text{Ba}_2\text{Ca}_{n-1}\text{Cu}_n\text{O}_{2n+3}$ ($n = 3, 4$). *Physica C* **226**, 222–226 (1994).
19. H. Kitō, A. Iyo, M. Hirai, A. Crisan, M. Tokumoto, S. Okayasu, M. Sasase, H. Ihara, Superconducting properties of the heavy-ions and neutron irradiated $(\text{Cu,C})\text{Ba}_2\text{Ca}_{n-1}\text{Cu}_n\text{O}_{2n+4-\delta}$ ($n = 3, 4$ and 5). *Physica C* **378–381**, 329–332 (2002).
20. Y. Shimakawa, J. D. Jorgensen, D. G. Hinks, H. Shaked, R. L. Hitterman, F. Izumi, T. Kawashima, E. Takayama-Muromachi, T. Kamiyama, Crystal structure of $(\text{Cu,C})\text{Ba}_2\text{Ca}_3\text{Cu}_4\text{O}_{11+\delta}$ ($T_c = 117$ K) by neutron-powder-diffraction analysis. *Phys. Rev. B* **50**, 16008–16014 (1994).

21. C. P. Bean, Magnetization of high-field superconductors. *Rev. Mod. Phys.* **36**, 31–39 (1964).
22. S. Yu, E. M. Kopnin, E. Takayama-Muromachi, Critical current densities and irreversibility fields of high- T_c superconductors $\text{AuBa}_2\text{Ca}_{n-1}\text{Cu}_n\text{O}_{2n+3}$ ($n=3, 4$) prepared under high pressure. *Sci. Technol. Adv. Mater.* **4**, 277–280 (2003).
23. M. Rupp, A. Gupta, C. C. Tsuei, Magnetic field induced broadening of the resistive transition in epitaxial c -axis-oriented $\text{HgBa}_2\text{CaCu}_2\text{O}_{6+\delta}$ films. *Appl. Phys. Lett.* **67**, 291–293 (1995).
24. Y. Moriwaki, T. Sugano, A. Tsukamoto, C. Gasser, K. Nakanishi, S. Adachi, K. Tanabe, Fabrication and properties of c -axis Hg -1223 superconducting thin films. *Physica C* **303**, 65–72 (1998).
25. P. M. Shirage, A. Iyo, D. D. Shivagan, A. Crisan, Y. Tanaka, Y. Kodama, H. Kito, Critical current densities and irreversibility fields of a $\text{HgBa}_2\text{Ca}_{n-1}\text{Cu}_n\text{O}_{2n+2+\delta}$ sample containing $n=6$ –15 phases. *Physica C* **468**, 1287–1290 (2008).
26. G. Brandstätter, F. M. Sauerzopf, H. W. Weber, Magnetic properties and critical currents in TI-based high- T_c superconducting single crystals. *Phys. Rev. B* **55**, 11693–11701 (1997).
27. M. Azuma, Z. Hiroi, M. Takano, Y. Bando, Y. Takeda, Superconductivity at 110 K in the infinite-layer compound $(\text{Sr}_{1-x}\text{Ca}_x)_{1-y}\text{CuO}_2$. *Nature* **356**, 775–776 (1992).
28. C. U. Jung, J. Y. Kim, M.-S. Kim, M.-S. Park, H.-J. Kim, Y. S. Yao, S. Y. Lee, S.-I. Lee, Synthesis and pinning properties of the infinite-layer superconductor $\text{Sr}_{0.9}\text{La}_{0.1}\text{CuO}_2$. *Physica C* **366**, 299–305 (2002).
29. Y. Iijima, N. Tanabe, O. Kohno, Y. Ikeno, Inplane aligned $\text{YBa}_2\text{Cu}_3\text{O}_{7-x}$ thin films deposited on polycrystalline metallic substrates. *Appl. Phys. Lett.* **60**, 769–771 (1992).
30. Y. Yamada, T. Muroga, H. Iwai, T. Watanabe, S. Miyata, Y. Shiohara, Progress of PLD and IBAD processes for YBCO wire in the SRL-Nagoya Coated Conductor Centre—New method for a coated conductor using a self-epitaxial PLD-CeO₂ buffer. *Supercond. Sci. Technol.* **17**, S70–S73 (2004).
31. A. Goyal, D. P. Norton, D. K. Christen, E. D. Specht, M. Paranthaman, D. M. Kroeger, J. D. Budai, Q. He, F. A. List, R. Feenstar, H. R. Kerchner, D. F. Lee, E. Hatfield, P. M. Martin, J. Mathis, C. Park, Epitaxial superconductors on rolling-assisted biaxially-textured substrates (RABiTS): A route towards high critical current density wire. *Appl. Supercond.* **4**, 403–427 (1996).
32. D. P. Norton, A. Goyal, J. D. Budai, D. K. Christen, D. M. Kroeger, E. D. Specht, Q. He, B. Saffian, M. Paranthaman, C. E. Klabunde, D. F. Lee, B. C. Sales, F. A. List, Epitaxial $\text{YBa}_2\text{Cu}_3\text{O}_7$ on biaxially textured nickel (001): An approach to superconducting tapes with high critical current density. *Science* **274**, 755–757 (1996).

Acknowledgments: We acknowledge the useful discussions with W. K. Kwok. **Funding:** This work was supported by National Key R&D Program of China (grant nos. 2016YFA0300401 and 2016YFA0401704) and National Natural Science Foundation of China (grant nos. A0402/11534005 and A0402/11674164). **Author contributions:** Y.Z. mainly performed the sample growth with the help of W.L., X.Z., H.Z., Z.H., and C.H. Y.Z. and H.-H.W. performed and analyzed the resistivity and magnetization. Y.Z. and X.Z. measured and analyzed the XRD. H.-H.W. and Y.Z. contributed to the writing of the paper. H.-H.W. initiated the original idea and coordinated the whole work. All authors have discussed results and interpretations. **Competing interests:** The authors declare that they have no competing interests. **Data and materials availability:** All data needed to evaluate the conclusions of the paper are present in the paper and/or the Supplementary Materials. Additional data related to this paper may be requested from the authors.

Submitted 28 April 2018

Accepted 21 August 2018

Published 28 September 2018

10.1126/sciadv.aau0192

Citation: Y. Zhang, W. Liu, X. Zhu, H. Zhao, Z. Hu, C. He, H.-H. Wen, Unprecedented high irreversibility line in the nontoxic cuprate superconductor $(\text{Cu,C})\text{Ba}_2\text{Ca}_3\text{Cu}_4\text{O}_{11+\delta}$. *Sci. Adv.* **4**, eaau0192 (2018).

Unprecedented high irreversibility line in the nontoxic cuprate superconductor $(\text{Cu,C})\text{Ba}_2\text{Ca}_3\text{Cu}_4\text{O}_{11+\delta}$

Yue Zhang, Wenhao Liu, Xiyu Zhu, Haonan Zhao, Zheng Hu, Chengping He and Hai-Hu Wen

Sci Adv 4 (9), eaau0192.
DOI: 10.1126/sciadv.aau0192

ARTICLE TOOLS	http://advances.sciencemag.org/content/4/9/eaau0192
SUPPLEMENTARY MATERIALS	http://advances.sciencemag.org/content/suppl/2018/09/24/4.9.eaau0192.DC1
REFERENCES	This article cites 32 articles, 1 of which you can access for free http://advances.sciencemag.org/content/4/9/eaau0192#BIBL
PERMISSIONS	http://www.sciencemag.org/help/reprints-and-permissions

Use of this article is subject to the [Terms of Service](#)